Observation of near-critical reflection of internal waves in a stably stratified fluid

Thierry Dauxois,[a] Anthony Didier, and Eric Falcon[b]
Laboratoire de Physique, École Normale Supérieure de Lyon, UMR-CNRS 5672, 46 allée d'Italie, 69007 Lyon, France

(Received 22 April 2003; accepted 10 February 2004; published online 29 April 2004)

An experimental study is reported of the near-critical reflection of internal gravity waves over sloping topography in a stratified fluid. An overturning instability close to the slope and triggering the boundary-mixing process is observed and characterized. These observations are found in good agreement with a recent nonlinear theory. © *2004 American Institute of Physics.*
[DOI: 10.1063/1.1711814]

I. INTRODUCTION

The reflection of near-critical internal waves over sloping topography plays a crucial role in determining exchanges between the coastal ocean and the adjacent deep waters. Direct measurements of mixing in the ocean, using tracers,[1] have vindicated decades of phenomenological and theoretical inferences. In particular, these measurements have shown that most of the vertical mixing is not taking place inside the ocean, but close to the boundaries and topographic features.[2] These results have directed attention to the possible role of internal wave reflection in the boundary-mixing process.

Internal waves have different properties of reflection from a rigid boundary than do sound or light waves.[3] Instead of following the familiar Snell's law, internal waves reflect off a boundary such that the angle with respect to gravity direction is preserved upon reflection (Fig. 1). This peculiar reflection law leads to a concentration of the reflected energy density into a narrow ray tube upon reflection as displayed in Fig. 1. Theoretical descriptions of this reflection process have been framed largely in terms of linear and stationary wave dynamics.[3,4] However, when the slope angle, γ, is equal to the incident wave angle, β, these restrictions lead to an unrealistic prediction: The reflected rays lie along the slope with an infinite amplitude and a vanishing group velocity. Theoretical results have recently healed this singularity by taking into account the role of transience and nonlinearity.[5]

Following preliminary oceanographic measurements,[6,7] Eriksen[8] has beautifully observed, near the bottom of a steep flank of a tall North Pacific Ocean seamount, an internal wave reflection process leading to a clear departure from a Garett–Munk model[9] for wave frequencies at which ray and bottom slopes match. Several experimental facilities[10–15] have therefore been dedicated to the understanding of the internal wave reflection and associated instabilities.

However, results of a controlled laboratory experiment close to the critical conditions are still lacking since previous ones with a moving paddle[10,11,13] at one end of a very long tank, or by the vibration of the tank itself,[14] does not generate a clear incident wave beam as needed for a careful study. In addition, a direct comparison with the recent and complete nonlinear theory near the critical reflection would be possible. Finally, the goal is to improve the understanding of the possible mixing mechanism near the sloping topography of ocean as very recently initiated by MacPhee and Kunze[16] by exhibiting the instability mechanisms leading to mixing. The paper is organized as follows. The experimental setup is described and carefully explained in Sec. II. The main experimental results are presented in Sec. III, and comparisons with the theory is also provided. Finally, Sec. IV contains conclusions and perspectives.

II. EXPERIMENTAL SETUP

The experimental setup consists of a 38 cm long Plexiglas tank, 10 cm wide, filled up to 22 cm height with a linearly salt-stratified water obtained by the ''double bucket'' method.[17] The choice of salt, sodium nitrate ($NaNO_3$) snow, is motivated due to its highly solubility in water leading to a salty water viscosity close to the fresh one. Moreover, this salt allows to reach a strong stratification: The fluid density $[1 \leqslant \rho(z) \leqslant 1.2\ \mathrm{g/cm^3}]$ measured at different altitudes $(22 \geqslant z > 0\ \mathrm{cm})$ by a conductimetric probe leads to a linear vertical density profile of slope $d\rho/dz \simeq -0.0104\ \mathrm{g/cm^4}$. A rectangular Plexiglas sheet, 3 mm thick and 9.6 cm wide (to allow exchange of water) is introduced at one end of the tank with an angle $\gamma = 35°$ with respect to the horizontal tank bottom (see Fig. 1) to create the reflective sloping boundary.

Internal waves are generated by a sinusoidal excitation provided by the vertical motion of a horizontal PVC plunging cylinder (3.1 cm in diameter and 9.4 cm long). The cylinder is located roughly midway between the base tank and the free surface. This wave maker is driven by an electromagnetic vibration exciter powered by a low frequency power supply. Optical measurements confirm[18] that the cylinder motion is sinusoidal without distortions for vibrational frequencies $0.2 \leqslant f \leqslant 0.5$ Hz and maximal displacement amplitudes, A_{pp}, up to 8.5 mm (peak to peak).

[a]Electronic mail: thierry.dauxois@ens-lyon.fr
[b]Electronic mail: eric.falcon@ens-lyon.fr

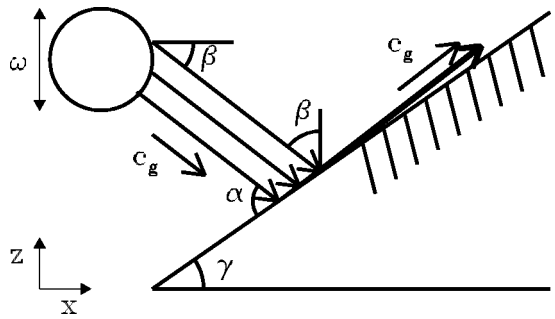

FIG. 1. Schematic view of the reflection process when the incident wave nearly satisfies the critical condition $\gamma \approx \beta$. The group velocity of the reflected wave makes a very shallow angle with the slope. c_g indicates the incident and reflected group velocities. The reflection law leads to a concentration of the energy density into a narrow ray tube.

The well-known and nonintuitive dispersion relation of internal waves in an incompressible, inviscid and linearly stratified fluid reads[19]

$$\omega = \pm N \frac{k_\perp}{|\mathbf{k}|} = \pm N \sin\beta, \tag{1}$$

where $k_\perp$ is the component of $\mathbf{k}$ perpendicular to the z axis, $N = \sqrt{-(g/\rho_0)\partial\rho/\partial z}$ is the constant buoyancy (or Brunt–Väisälä) frequency, $\rho(z)$ the fluid density at altitude z, $g = 981$ cm/s^2 the acceleration of gravity, and $\rho_0 \simeq 1$ g/cm^3 a reference density. Thus, from Eq. (1), the wave frequency, $\omega = 2\pi f$, determines the inclination angle β of the phase surfaces with the vertical, and not the magnitude of the wave vector $\mathbf{k}$. From Eq. (1), β is also the angle between the group velocity $\mathbf{c}_g = \partial\omega/\partial\mathbf{k}$ and the horizontal, since $\mathbf{c}_g \perp \mathbf{k}$. Thus, for a given stratification and frequency, internal waves of low (higher) frequency propagate at low (steeper) angle.

The outward radiation of energy is thus along four beams oriented at an angle β with the horizontal, the familiar St. Andrews Cross structure.[20] The beam propagating directly toward the slope has been singled out by adding a grid on the surface of water. This grid strongly damps the three other wave beams that propagate towards the free surface, and thereby prevents reflection of such beams. A planar wave pattern consisting of parallel rays is thus generated from the wave maker. Although it is well-known that the spatial spectrum of waves generated by an oscillating cylinder is large,[15,21,22] it has been experimentally checked that the dominant wavelength is approximately equal to the cylinder diameter (see later). Moreover, measurements confirm that the low vibrational amplitudes of cylinder do not strongly influence the wavelength generated.

Different visualization methods are used to study the reflection mechanism of such internal gravity waves by a boundary layer. First, the usual shadowgraph technique[23] allows visualization of the qualitative and global two-dimensional evolution of the incident and reflected waves. It involves projecting a point source of light through stratified water onto a screen behind the tank. The optical refractive index variations induced by the fluid density variations, allows one to observe isodensity lines (or isopycnals) on the screen, located perpendicularly to the light source and parallel to the longest wall tank. It is therefore possible to measure the group velocity angle, β, and the phase velocity v_φ of the incident wave. For various frequencies of excitation, $0.2 \leqslant f \leqslant 0.5$ Hz, the angle β of the St. Andrews Cross is measured on a screen leading to a linear relation between ω and $\sin\beta$ as predicted by Eq. (1) with a slope of $N = 3.1 \pm 0.1$ rad/s, for the stratified fluid prepared as earlier. This value is in good agreement with the earlier static one obtained from the density profile with a conductimetric probe. The cutoff frequency is then $f_c = N/(2\pi) \simeq 0.5$ Hz. By time of flight measurements between signals delivered by two photodiodes, 1 cm apart, each of 7 mm^2 area, located behind the tank along the propagation direction, a value $v_\varphi = 0.6 \pm 0.4$ cm/s was obtained for an excitation frequency $f = 0.25$ Hz. When these signals are crosscorrelated by means of a spectrum analyzer, the averaged dephasing time leads to $v_\varphi = 0.7 \pm 0.3$ cm/s, close to the previous value. The wavelength of the incident wave is thus $\lambda = v_\varphi / f \simeq 3$ cm, corresponding as expected to the oscillating cylinder's diameter. However, neither this shadowgraph technique nor one[23] using passive tracers (fluorescein dye) is sufficiently sensitive to observe quantitative and local internal wave properties closed to the reflective boundary layer.

Accordingly, the classical Schlieren method[23,24] of visualization has been used. Let us just note that behind the tank, the light beam is refocused by a lens a small distance after a slit (instead of the usual knife blade to increase contrast) to filter the rays. The slit is oriented orthogonally to the slope generating straight horizontal fringe lines in the case of no excitation. The image of the observation field (strongly dependent of the 7.5 cm diameter lens) is focused on the screen by a last lens. The internal wave, producing density disturbances, causes lines to distort, this distorting line pattern being recorded by a camera. Note that this experimental technique is sensitive to the index gradient, and therefore to the density gradient, *orthogonal* to the slit, i.e., parallel to the slope.

III. EXPERIMENTAL RESULTS AND COMPARISON WITH THEORY

The Schlieren technique allows one to carefully observe quantitative and local internal wave properties during the reflection process. Critical reflection arises when an incident wave beam with an angle of propagation β reflects off the slope of angle $\gamma \simeq \beta$, the reflected wave being then trapped along the plane slope. This corresponds to a critical frequency $f_c = N \sin\gamma \simeq 0.28 \pm 0.01$ Hz, N being equal to 3.1 ± 0.1 rad/s for all experiments. It is possible to observe that the isodensity lines (isopycnals), initially horizontal without excitation, are bent for an excitation near f_c ($0.78 \leqslant f/f_c \leqslant 1.14$), and fold over themselves along the length of the slope. Figure 2 shows a time sequence of constant density surfaces, depicting sequential snapshots of the flow throughout one period of its development.

These pictures strikingly show the distortion of the isopycnals in the slightly subcritical case with $f/f_c = 0.78$. In panel (a), the density disturbance is very small and one can observe essentially the initial horizontal background stratifi-

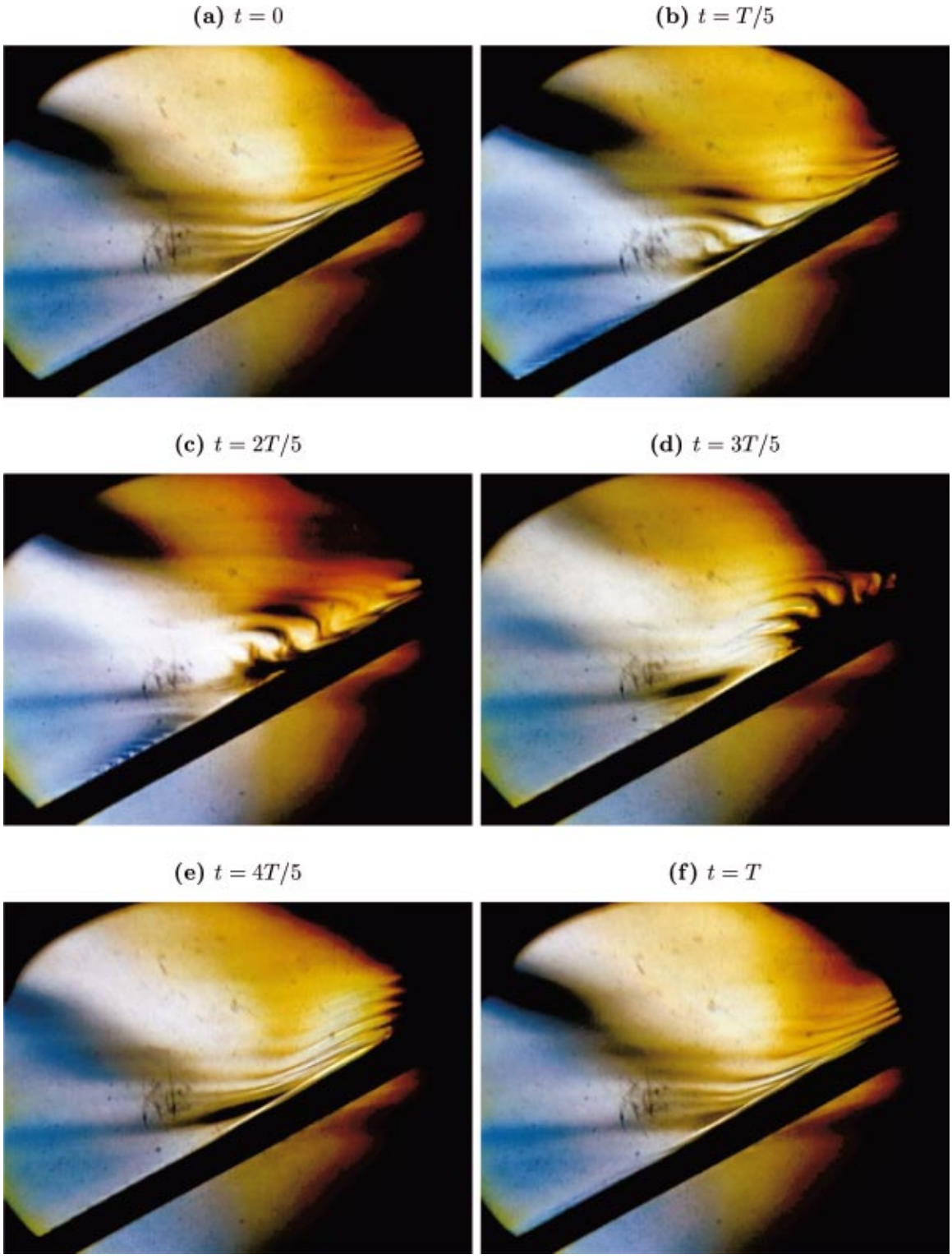

FIG. 2. (Color) Schlieren pictures showing the slightly subcritical reflection ($f/f_c=0.78$) of an internal wave on a slope, during one incident wave period T. The slope (thick black line) has an angle $\gamma=35°$. The incident wave plane comes in from the left (inclined black region near the top left corner between blue and yellow regions). The reflected wave plane is hardly noticeable. Wave maker vibrational frequency and peak to peak amplitude are, respectively, $f=0.22$ Hz and $A_{pp}=6.7$ mm.

cation. This background stratification, usually obtained with dye fluorescein, should be invisible with this Schlieren method. However, as previously reported by MacPhee and Kunze,[16] the comparison between shadowgraph and fluorescein dye visualizations allows to identify these lines with isopycnals. In panel (b), the disturbance generated by the incident wave breaking against the slope begins to ''fold-up'' the isopycnals. As time progresses [see panel (c)], wave overturning develops around a front: The buoyancy becomes statically unstable. This overturned region climbs along the

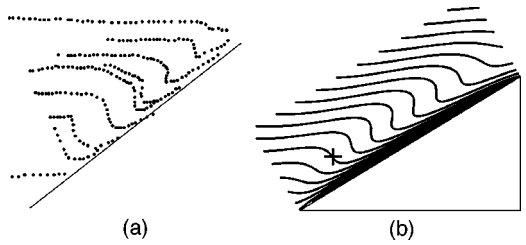

FIG. 3. (a) Experimental isopycnals extracted from a region of Fig. 2(c). (b) Theoretical isopycnals from Eq. (2). The star indicates the position of the front.

slope as time continues, and the folded isopycnals collapse into turbulence that mixes the density field within the breaking region [see panel (d)]. The maximum thickness of this reflected disturbance is of the order of 5 mm, and decreases with time as theoretically predicted.[5] Finally, the flow begins to relaminarize [panel (e)]. One can check that panels (a) and (f) are almost identical, showing that the flow is entirely restratified [panel (f)] after one period of excitation.

Figure 2 has been analyzed with an image processing software (Scion-Image) to extract the isopycnals from the pictures. A typical experimental result for the distortion of isopycnals is reported in Fig. 3(a), and is compared with a theoretical result in Fig. 3(b). The analytic solution of the density field of the initial value problem in the critical case reads[5]

$$\rho=\rho_0\left\{1-\frac{N^2}{g}\left[z\cos\gamma-\psi B\sqrt{\frac{|\mathbf{k}|\sin^2(2\beta)}{2\omega_+}}\right]\right\}, \tag{2}$$

where

$$B=\sqrt{\frac{t}{z}}J_1\sin[\omega_+ t-|\mathbf{k}|\sin(\beta+\gamma)x], \tag{3}$$

$$J_1\equiv J_1(2\sqrt{2\omega_+\cos^2\beta|\mathbf{k}|tz}), \tag{4}$$

$J_1(\cdot)$ being the Bessel function, ω_+ is the positive solution of Eq. (1), ψ is the maximum amplitude of the streamfunction, and x is the horizontal coordinate. Figure 3 shows a good qualitative agreement between experimental and theoretical results, the value for the time t being arbitrarily chosen. Far from the slope, the density disturbance is very small and one sees essentially the initial background stratification. Closer to the slope, the disturbance folds up the isopycnals, and this produces a region of static instability.

Recording several isopycnals and using image processing, it is also possible to follow the temporal evolution of a *single isopycnal* during its overturning. As this phenomenon is periodic with a period $T=1/f$, it is possible to reconstruct from this temporal evolution the density profile picture at a given time t. This allows one to follow the position, and therefore the propagation velocity of the front along the slope at different times. The front is defined as the inflexion point [represented by the star in Fig. 3(b)] of the followed isopycnal. Figure 4(a) shows, during two periods, the isopycnal front position, x_f, along the slope as a function of time. The periodic evolution of this front position is clearly observed, and the local slope of the curves in Fig. 4(a) allows one to roughly measure the front velocity, v_f, as a function of time, as reported in Fig. 4(b).

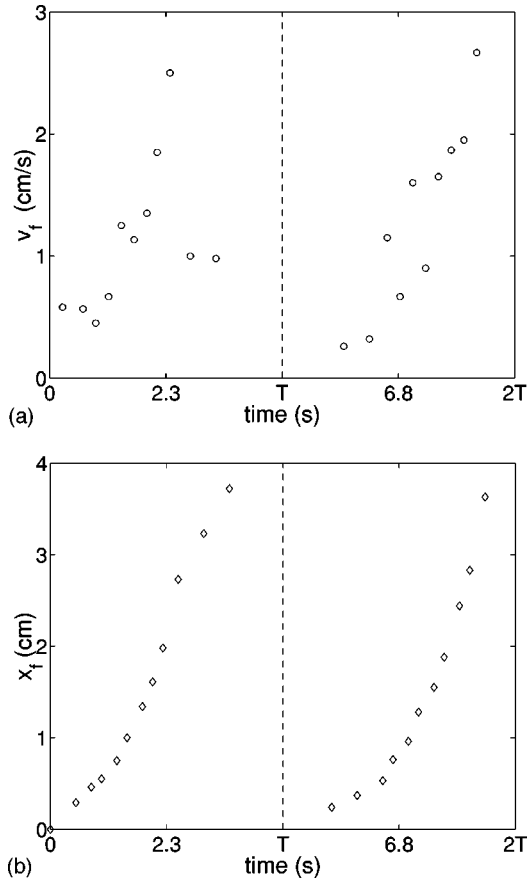

FIG. 4. Temporal evolution of the isopycnal front position (a) and velocity (b) along the slope, during two periods of vibration. $T\simeq 4.5$ s, $f/f_c=0.78$, and $A_{pp}=6.7$ mm.

The front velocity from its creation to its collapsing increases from 0.5 up to 3 cm/s. The front has thus travelled roughly 4 cm in one period ($\sim$4.5 s). This leads to an averaged front velocity in agreement with the phase speed measurement obtained from the shadowgraph visualizations (see Sec. II).

The wave maker frequency is now increased up to $f=0.32$ Hz, to have an incident plane wave tilted with an angle β steeper than the slope angle γ. In this slightly supercritical case ($f/f_c=1.14$), intrusions are still observed, but the density field does not fold up so abruptly and does not lead anymore to overturning instability (see Fig. 5). Except the value of the frequency f, all others parameter values have been kept identical to the ones in Fig. 2. The instant of this snapshot has been chosen when the isopycnal distortion is the largest. This distortion is clearly far from leading to an overturning instability as encountered in the subcritical case of Fig. 2(c): The reflected wave is not trapped along the slope in the boundary layer, and consequently the isopycnals are not overturned. Moreover the density front velocity is measured roughly constant, 0.5 cm/s, during two periods of vibration. Both differences confirm that the singularity appears only in the critical case.[5]

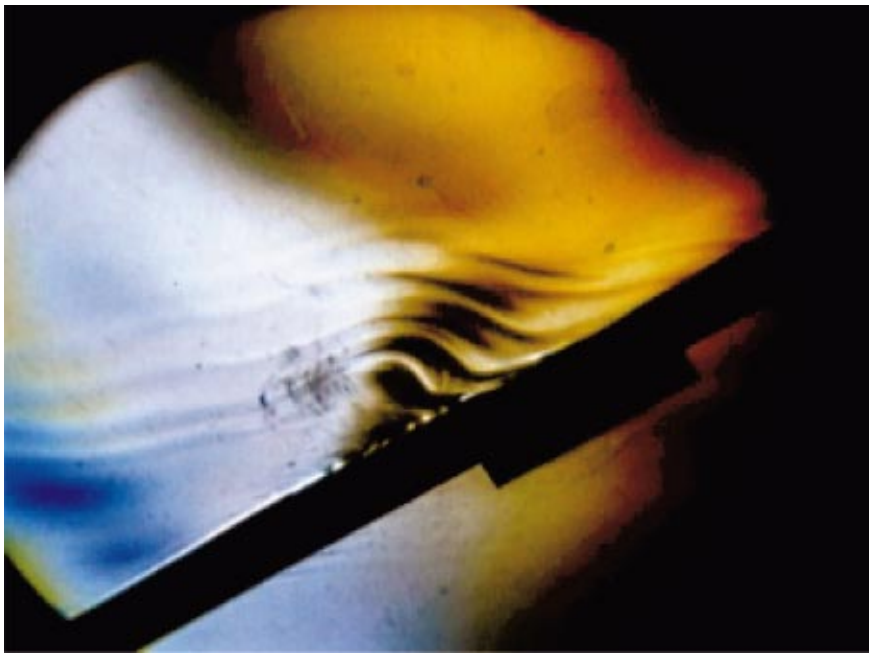

FIG. 5. (Color) Schlieren picture showing the isodensity lines during the slightly supercritical reflection ($f/f_c=1.14$) of an internal wave on a slope. The slope (thick black line) has an angle $\gamma=35°$. The incident wave plane comes in from the left (inclined white region near the top left corner between blue and yellow regions). The reflected wave plane is hardly noticeable. Vibrational parameters: $f=0.32$ Hz and $A_{pp}=6.7$ mm. This picture should be compared with Fig. 2(c).

IV. CONCLUSIONS AND PERSPECTIVES

The Schlieren technique allows us to study the spatiotemporal evolution of the internal waves reflection close to the critical reflection, where nonlinear processes occur. The dynamics of isopycnals is then found in agreement with a recent nonlinear theory.[5] Moreover, this experiment confirms the theoretically predicted scenario for the transition to boundary-layer turbulence responsible for boundary mixing: The growth of a density perturbation produces a statically unstable density field which then overturns with small-scale fluctuations inside.[16] Panel (d) of Fig. 2 is characteristic of the onset of turbulence triggered by overturning instability near the slope.

This turbulent mechanism is likely responsible for the formation of highly ''stepped'' temperature profiles near steep slopes in lakes.[25] Moreover, the formation of suspended sediment layers, called nepheloid layers, at continental slopes has been linked to critical angle reflection of internal waves,[16,26] and suggests that this reflection process plays an important role in the seawards transport of sediments in the fluid. A possible extension of this work, with a smaller slope angle to be closer to real oceanographic situations, would be to study and characterize the long time behavior and diffusion process of such particle layers toward the fluid interior.

ACKNOWLEDGMENTS

The authors warmly thank J.-C. Géminard and J. Sommeria for helpful suggestions. This work has been partially supported by the French Ministère de la Recherche grant ACI jeune chercheur-2001 No. 21-31.

[1] J. R. Ledwell, A. J. Watson, and C. S. Law, ''Evidence for slow mixing across the pycnocline from an open ocean tracer release experiment,'' Nature (London) **364**, 701 (1993).
[2] K. L. Polzin, J. M. Toole, J. R. Ledwell, and R. W. Schmitt, ''Spatial variability of turbulent mixing in the abyssal ocean,'' Science **76**, 93 (1997).
[3] O. M. Phillips, *The Dynamics of the Upper Ocean* (Cambridge University Press, Cambridge, 1966).
[4] D. A. Gilbert, ''Search for evidence of critical internal wave reflection on the continental rise and slope off Nova Scotia,'' Atmos.-Ocean. **31**, 99 (1993).
[5] T. Dauxois and W. R. Young, ''Near-critical reflection of internal waves,'' J. Fluid Mech. **390**, 271 (1999).
[6] H. Sandstrom, ''The importance of the topography in generation and propagation of internal waves,'' Ph.D. thesis, University of California, San Diego, La Jolla, 1966.
[7] C. C. Eriksen, ''Observations of internal wave reflection off sloping bottoms,'' J. Geophys. Res. **87**, 525 (1982); ''Implications of ocean bottom reflection for internal wave spectra and mixing,'' J. Phys. Oceanogr. **15**, 1145 (1985).
[8] C. C. Eriksen, ''Internal wave reflection and mixing at Fieberling Guyot,'' J. Geophys. Res. **103**, 2977 (1998).
[9] C. Garett and W. Munk, ''Internal waves in the ocean,'' Annu. Rev. Fluid Mech. **11**, 339 (1979).
[10] S. A. Thorpe, ''On the reflection of a strain of finite-amplitude internal waves from a uniform slope,'' J. Fluid Mech. **178**, 279 (1987).
[11] D. Cacchione and C. Wunsch, ''Experimental study of internal waves over a slope,'' J. Fluid Mech. **66**, 223 (1974).
[12] I. P. D. De Silva, J. Imberger, and G. N. Ivey, ''Localized mixing due to a breaking internal wave ray at a sloping bed,'' J. Fluid Mech. **350**, 1 (1997).
[13] G. N. Ivey and R. I. Nokes, ''Vertical mixing due to the breaking of critical internal waves on sloping boundaries,'' J. Fluid Mech. **204**, 479 (1989).
[14] L. R. M. Maas, D. Benielli, J. Sommeria, and F.-P. A. Lam, ''Observation of an internal wave attractor in a confined stably stratified fluid,'' Nature (London) **388**, 557 (1997).
[15] B. R. Sutherland, G. O. Hughes, S. B. Dalziel, and P. F. Linden, ''Internal waves revisited,'' Dyn. Atmos. Oceans **31**, 209 (2000); B. R. Sutherland, S. B. Dalziel, G. O. Hughes, and P. F. Linden, ''Visualization and measurement of internal waves by 'synthetic Schlieren.' Part 1. Vertically oscillating cylinder,'' J. Fluid Mech. **390**, 93 (1999).
[16] E. E. McPhee-Shaw and E. Kunze, ''Boundary layer intrusions from a sloping bottom: A mechanism for generating intermediate nepheloid layers,'' J. Geophys. Res. **107**, 10.1029 (2002).
[17] G. Oster, ''Density gradients,'' Sci. Am. **213**, 70 (1965); D. F. Hill, ''General density gradients in general domains: The 'two-tank' method revisited,'' Exp. Fluids **32**, 434 (2002).
[18] A. Didier, DEA Report, ENS Lyon, 2002 (in French).
[19] J. Lighthill, *Waves in Fluids* (Cambridge University Press, Cambridge, 1978).

[20]D. E. Mowbray and B. S. H. Rarity, ''A theoretical and experimental investigation of the phase configuration of internal waves of small amplitude in a density stratified liquid,'' J. Fluid Mech. **28**, 1 (1967).
[21]J. C. Appleby and D. G. Crighton, ''Internal gravity waves generated by oscillations of a sphere,'' J. Fluid Mech. **183**, 439 (1987).
[22]B. Voisin, ''Limit state of internal wave beams,'' J. Fluid Mech. **496**, 243 (2003).
[23]W. Merzkirch, *Flow Visualization* (Academic, New York, 1974).
[24]S. B. Dalziel, G. O. Hughes, and B. R. Sutherland, ''Whole-field density measurements by 'synthetic Schlieren,' '' Exp. Fluids **28**, 322 (2000); F. Peters, ''Schlieren interferometry applied to a gravity wave in a density-stratified liquid,'' *ibid.* **3**, 261 (1985).
[25]D. R. Caldwell, J. M. Brubaker, and V. T. Neal, ''Thermal microstructure on a lake slope,'' Limnol. Oceanogr. **23**, 372 (1978).
[26]S. A. Thorpe and M. White, ''A deep intermediate nepheloid layer,'' Deep-Sea Res., Part A **35**, 1665 (1988).